

Interaction Model for Anthracycline Activity against DNA Topoisomerase II[†]

Stefano Moro,^{*,§} Giovanni L. Beretta,^{‡,§,||} Diego Dal Ben,[#] John Nitiss,[⊥] Manlio Palumbo,[#] and Giovanni Capranico^{*,‡}

G. Moruzzi Department of Biochemistry, Alma Mater Studiorum University of Bologna, Via Irnerio 48, Bologna, Italy, Department of Pharmaceutical Sciences, University of Padova, Via Marzolo 5, Padova, Italy, and Department of Pharmacology, St. Jude's Children's Hospital, 332 North Lauderdale, Memphis, Tennessee 38105

Received December 2, 2003; Revised Manuscript Received March 18, 2004

ABSTRACT: DNA topoisomerase II (Top2) is an essential nuclear enzyme and a target of very effective anticancer drugs including anthracycline antibiotics. Even though several aspects of drug activity against Top2 are understood, the drug receptor site is not yet known. Several Top2 mutants have altered drug sensitivity and have provided information of structural features determining drug action. Here, we have investigated the sensitivity to three closely related anthracycline derivatives of yeast Top2 bearing mutations in the CAP-like domain and integrated the findings with computer models of ternary drug–enzyme–DNA complexes. The results suggest a model for the anthracycline receptor wherein a drug molecule has specific interactions with the cleaved DNA as well as amino acid residues of the CAP-like domain of an enzyme monomer. The drug molecule is intercalated into DNA at the site of cleavage, and interestingly, drug–enzyme contacts involve one side of the four-ring chromophore and the side chain of the anthracycline molecule. The findings may explain several established structure–activity relationships of antitumor anthracyclines and may thus provide a framework for further developments of effective Top2 poisons.

DNA topoisomerases are essential enzymes, present in all organisms (1–3). They modify the nucleic acid topology in connection with a number of nuclear processes such as replication, transcription, chromatin remodeling, chromosome condensation/decondensation, recombination, and repair (2, 4). All DNA topoisomerases can introduce breaks into DNA segments and Top2¹ transport a double helix through a double-stranded cut of another duplex. Two isoforms of Top2 (α and β) are encoded in the human genome, whereas one Top2 enzyme is present in *Saccharomyces cerevisiae*. Topoisomerase activity can however be harmful to cells due to the action of small compounds (5–8), known as topoisomerase poisons, which include effective antitumor drugs. The compounds transform these essential enzymes into lethal DNA-damaging agents by stabilizing an enzyme–DNA complex wherein DNA strands are cut and covalently linked to the enzyme (5, 6, 9). Anthracycline antibiotics such as DOX, DNR, and related agents were isolated from *Streptomyces* species and are among the most effective Top2 poisons. DOX and closely related derivatives have clinical applications in front-line therapies of several solid tumors, lymphomas, and leukemias. The parent drugs, DOX and

DNR, have a characteristic four-ring structure (rings A–D) that is linked, via a glycoside bond, to an amino sugar, daunosamine (Figure 1). The only difference between the parent drugs is at the C-9 side chain of ring A, with DOX being the C-14 hydroxyl derivative of DNR (Figure 1).

Knowledge of the mechanism of action of anticancer poisons has been gained by several lines of research. The definition of the sequence specificity of Top2 poisons strongly suggested a stacking model in which the poison molecule intercalates between DNA base pairs at the DNA/protein interface of the enzyme active site (8, 10). The model has been supported by other experimental evidence including drug photoaffinity labeling of DNA, base mismatch effects, drug binding findings, covalently DNA-bound intercalating agents, and others (6, 11–13). Similar models have been proposed for CPT, a specific poison of Top1 (6, 14), and the recent resolution of the ternary DNA–drug–Top1 complex (15) has provided final evidence for an intercalation model of a Top1 poison. In the study (15), the authors showed that a topotecan molecule (a CPT analogue) is intercalated into the DNA at the site of cleavage contacting nucleotide as well as amino acid residues. The compound interferes with the catalytic reaction by displacing the DNA strand downstream to the cut, thus preventing strand religation (15). In the case of Top2, a crystal of a similar ternary complex still remains to be solved.

Important structural knowledge has been gained from several drug-resistant or drug-sensitive Top2 mutants (16, 17). Even though mutations were found in distinct protein domains, several mutations cluster at the $\alpha 4$ helix of the CAP-like domain of Top2 that was suggested to be important for binding of Top2 to the G (gate) DNA segment (18). Molecular analyses of such mutants indicated that the

[†] This work was supported by grants from the Associazione Italiana per la Ricerca sul Cancro (AIRC), Milan, and the PRIN program of Ministero dell'Istruzione, dell'Università e della Ricerca, Rome, Italy.

* Corresponding author e-mail: giovanni.capranico@unibo.it.

[‡] Alma Mater Studiorum University of Bologna.

[§] These authors contributed equally to the work.

^{||} Present address: Istituto Nazionale per lo Studio e la Cura dei Tumori, Via Venezian 1, Milan, Italy.

[⊥] St. Jude's Children's Hospital.

[#] University of Padova.

¹ Abbreviations: Top2, topoisomerase II; Top1, topoisomerase I; DOX, doxorubicin (adriamycin); DNR, daunorubicin (daunomycin); IDA, idarubicin (4-demethoxy-DNR); CPT, camptothecin.

conserved CAP-like domain has a critical role in both DNA site recognition and possibly binding of drugs to the Top2–DNA complex (19–23). S740W and T744P are among the most studied mutations at the $\alpha 4$ helix of the Cap-like domain (21, 22, 24). Yeast Top2 Ser-740 is homologous to Ser-83 of gyrA, which is frequently mutated in clinical or laboratory isolates of quinolone-resistant bacterial strains. Interestingly, GyrA bearing Ser-83 mutations had wild-type enzymatic activity and showed instead decreased affinity for fluoroquinolones (25). Resistance of Top2 mutants to anthracyclines has been studied much less than resistance to other anticancer poisons. In one study, selection of randomly mutated plasmid-borne yeast TOP2 gene provided evidence that G748E and A642S can confer DOX resistance to yeast Top2 (26). Interestingly, Gly-748 lies at one end of the $\alpha 4$ helix in the CAP-like domain. However, drug interactions relevant to anthracycline activity remain to be established.

Thus, to identify a putative anthracycline receptor and critical structural interactions of the drug in the ternary complex, we have studied two yeast Top2 mutants by integrating biochemical assays and computer molecular simulations. The sensitivity of yeast Top2 mutants to a homologous set of anthracycline derivatives was determined to establish sound structure–function relationships. The findings indicate a drug interaction model for anthracyclines that explains several published structure–activity relationships and can be of great value in understanding how current anticancer anthracyclines act and in rationally designing more effective Top2 poisons.

EXPERIMENTAL PROCEDURES

DNA Cleavage Assay. Wt and mutant Top2 enzymes have been purified as reported previously (24, 27). Anthracycline derivatives were kindly provided by Dr. A. Suarato (Upjohn-Pharmacia, Nerviano, Italy). DNA cleavage assay has been described already (27). Briefly, Simian virus 40 DNA was first restricted with *Eco*RI and then 5′-end-labeled with T4 kinase and [γ - 32 P]ATP. After phenol–chloroform extraction and ethanol precipitation, DNA was digested with a second restriction enzyme. Then, uniquely 5′-end-labeled DNA fragments were purified by agarose gel electrophoresis and electroelution. DNA was incubated with purified Top2, at similar enzyme activity, in a total volume of 20 μ L with or without drugs at the indicated concentrations in 10 mM Tris-HCl, pH 7.5, 45 mM KCl, 5 mM MgCl₂, 1 mM ATP, 2 mM DTT, 0.1 mM Na₂EDTA, and 15 μ g/mL BSA for 30 min at 37 °C. Reactions were stopped by adding of 1% SDS, 0.5 mg/mL proteinase K, and followed by 45 min at 45 °C. DNA cleavage was analyzed with 1% agarose gel in 89 mM Tris-base, 89 mM boric acid, and 2 mM Na₂EDTA or by sequencing gels. Dried gels were then exposed to Amersham Hyperfilm MP at –70 °C with intensifying screens. DNA cleavage extent was determined by densitometric analyses of autoradiograms.

Computational Methodologies. The coordinates for the 92-kDa wild-type yeast DNA topoisomerase II structure were from the Brookhaven Protein Data Bank (accession number: 1bgw). Missing crystallographic hydrogen atoms were added to topoisomerase protein structure using Molecular Operating Environment (MOE, ver.2002.03) software (Chemical Computing Group, Inc., Montreal, Canada). The positions of all

hydrogen atoms were optimized to a conjugate gradient (CG) of 0.1 kcal/mol·Å using the AMBER94 force field, with the atomic charges specified by the same force field (28). Hydrogen optimization was performed by first holding the positions of all non-hydrogen atoms fixed. Then, Top2–DNA covalent complex was built using MOE tools, introducing several major modifications to the original crystallographic coordinates since the PDB crystal structure does not include DNA. To obtain a plausible geometry of the enzyme–DNA covalent complex, we have edited the original coordinates removing the peptide sequence from Glu430 until Leu680, creating therefore enough space to accommodate a DNA oligomer in its canonical B-form. A complementary electrostatic potential field analysis has been used to appropriately locate the DNA structure on the truncated Top2. Then, we have rebuilt the peptide Glu430 to Leu680 by using an homology modeling technique implemented by MOE and the secondary and tertiary structure of Top2 around the DNA duplex.

Following MOE-homology modeling approach, independent models of the protein structure were been built using a Boltzmann-weighted randomized modeling procedure adapted from Levitt, combined with specialized logic for the proper handling of insertions and deletions. Each of these intermediate models was evaluated by a residue packing quality function, which is sensitive to the degree to which nonpolar side chain groups are buried and hydrogen bonding opportunities are satisfied. After data collection was complete, a library of independent models was created. Loops were modeled first, in random order. For each loop, a contact energy function analyzed the list of collected candidates, taking into account all atoms modeled already and any atoms specified by the user as belonging to the model environment (i.e., a ligand bound to the template). These energies were then used to make a Boltzmann-weighted choice of the candidates, the coordinates of which were then copied to the model. Any missing side chain atoms were modeled using the same procedure. Side chains of residues that had been copied from a template were modeled first, followed by side chains of modeled loops. Outgaps and their side chains were modeled last. A final model was built and minimized. The coordinates of the final model were generated either as the average of atom coordinates of intermediate models or as the coordinates of the intermediate model that scored best according to the packing quality function. Once the homology modeling procedure had finished, the final model was inspected using MOE's Stereochemical Quality Evaluation tools in order to confirm that the model stereochemistry was reasonably consistent with typical values found in crystal structures. In case of persistent problems, which might suggest a difficulty with the alignment used to build the model, then manual adjustments to the alignment was needed followed by a rebuilding of the model. This was particularly the case of loop areas. A poly-CG or a [CGCGATCGCG]₂ sequence was used to simulate the Top2–DNA covalent complex.

The entire complex was minimized to a conjugate gradient (CG) of 0.1 kcal/mol·Å using the AMBER94 force field, with the atomic charges on both protein and DNA being specified by AMBER94. The appropriate atomic charges of the phosphotyrosine moiety were calculated based on the fitting of the electrostatic potential using the RHF/AM1

formalism. All quantum mechanic calculations have been performed using Spartan O2 software (Wavefunction Inc., Irvine, CA). For the construction of the two Top2 mutants, Ser740 and Thr744 were replaced with Trp and Pro, respectively, using the Mutate module of the MOE. Both S740W and T744P mutants were subjected to a 250-ps simulation (1-fs time step) at 300 K following a 40-ps equilibration cycle. All dynamics were performed using NTP protocol implemented in MOE. Implicit solvation was taken into account during the dynamics using GA/SB approach (28). The resulting structures were averaged and energy minimized to a CG of 0.1 kcal/mol·Å using the AMBER94 force field.

Drug structures were fully optimized without geometry constraints using RHF/AM1 semiempirical calculations. The drugs were docked into the hypothetical binding site by using the MOE-Dock program, part of the MOE suite. Partial atomic charges for the ligands were imported from the Spartan output files. The program incorporated the use of manual and automatic docking procedures in combination with molecular mechanics within the Simulations module of MOE. The docking method enabled nonbonded van der Waals and electrostatic interactions to be simultaneously monitored during the docking, and several possible conformations for the ligand were evaluated interactively. “Flexible” ligand docking was then used to define the lowest energy position of each ligand using a Monte Carlo/annealing-based automated docking protocol, which used a random iterative algorithm to sample changes in torsion angles and atomic positions while simultaneously recalculating internal and interaction energies. The automated docking procedure then selected the best structures and subjected the totality of the binding site. During the docking, all torsion angles of side chains of the ligand were allowed to vary. The lowest energy complex resulting from each docking procedure was itself energy-minimized using MMFF94 (29, 30) to a gradient of 1.0 kcal/mol·Å. A 12-Å sphere about the drug molecule was further optimized to a gradient of 0.001 kcal/mol·Å. Complexes were ranked using the interaction energy (E_{int}) as the scoring function, with the interaction energy being the sum of the nonbonding interactions [i.e., van der Waals (E_{vdw}) and electrostatic (E_{elec}) contributions] of the complex. E_{int} did not calculate thermodynamic quantities and could be used only to compare relative stability of complexes. Thus, the interaction energy values could not be used to measure binding affinities since entropy changes and solvation effects were not taken into account.

RESULTS

Yeast Top2 Sensitivity to Antitumor Anthracyclines. We studied the molecular effects of anthracycline derivatives, IDA, dh-IDA-OH, and da-IDA (Figure 1), on yeast wild-type Top2 (wt yTop2) and two yTop2 mutants, S740W and T744P, known to have altered sensitivity to other top2 poisons (19, 24). IDA and da-IDA are derivatives of DNR, whereas dh-IDA-OH is a DOX analogue (Figure 1). The three studied anthracyclines were the most potent analogues known in stimulating DNA cleavage mediated by Top2 (8, 31). IDA has the same sequence specificity of parent drug DOX, whereas dh-IDA-OH and da-IDA have been shown to display somewhat different cleavage intensity patterns in sequencing gels (31). Drug sensitivity and site preferences

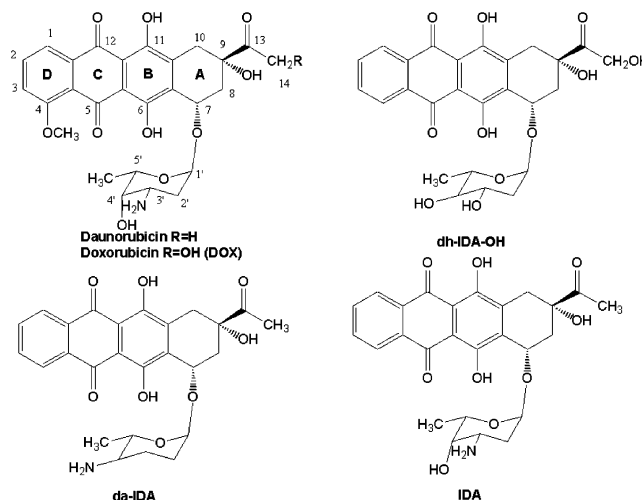


FIGURE 1: Chemical structures of the studied anthracycline derivatives.

of yeast mutants were investigated with a DNA cleavage assay by using SV40 DNA fragments.

Poison-sensitivity of wt yTop2 was initially compared to that of recombinant human Top2 α . The two enzymes were tested at similar activity with a cleavage assay (Figure 2). The wt yTop2 was slightly less sensitive than Top2 α to 50 μ M VM-26 (Figure 2) and to the other studied agents (not shown). Cleavage intensity patterns were somewhat different between yeast and human Top2 in the presence of VM-26, since fewer sites were selected by yTop2 than Top2 α (Figure 2). On the other hand, cleavage patterns were similar for anthracyclines whereas they varied for *m*-AMSA by comparing the two enzymes (not shown). In the presence of VM-26, uncut DNA was about 45–60%, 0–2%, and 30–40% with wt, S740W, and T744P yTop2, respectively (Figures 2 and 3). Thus, in agreement with previous findings (19), the results showed that S740W mutant was much more sensitive to VM-26 than wt yTop2 and T744P mutant.

Then, wt yTop2 was compared to yTop2 mutants by investigating double-stranded cleavage of SV40 DNA stimulated by the studied anthracycline derivatives, *m*-AMSA or VM-26 (Figure 3). The two mutants were both resistant to anthracyclines; however, they displayed somewhat distinct patterns. S740W mutant was completely resistant to the tested anthracycline analogues while being also resistant to *m*-AMSA and more sensitive to VM-26 (19). It must be noted that S740W appears to be much more resistant to anthracyclines than amsacrine (Figures 3 and 4). T744P mutant somewhat differed from the S740W mutation relative to anthracycline activity. T744P Top2 was completely resistant to IDA and da-IDA, whereas it was resistant to dh-IDA-OH to a lesser extent since dh-IDA-OH could stimulate some DNA cleavage in contrast to the other drug analogues (Figure 3, lanes Dh). In agreement with other reports (19), the T744P Top2 mutant was much more sensitive to *m*-AMSA (uncut DNA was 65%, 80%, and 10–20% with wt, S740W, and T744P yTop2, respectively) and slightly more sensitive to VM-26 (see above; Figures 3 and 4).

Drug-stimulated DNA cleavage patterns were also studied with sequencing gels (Figure 4). In agreement with previous findings on human Top2 isoforms (31), the three anthracyclines stimulated DNA cleavage with somewhat different site preferences: dh-IDA-OH increased strand cleavage at

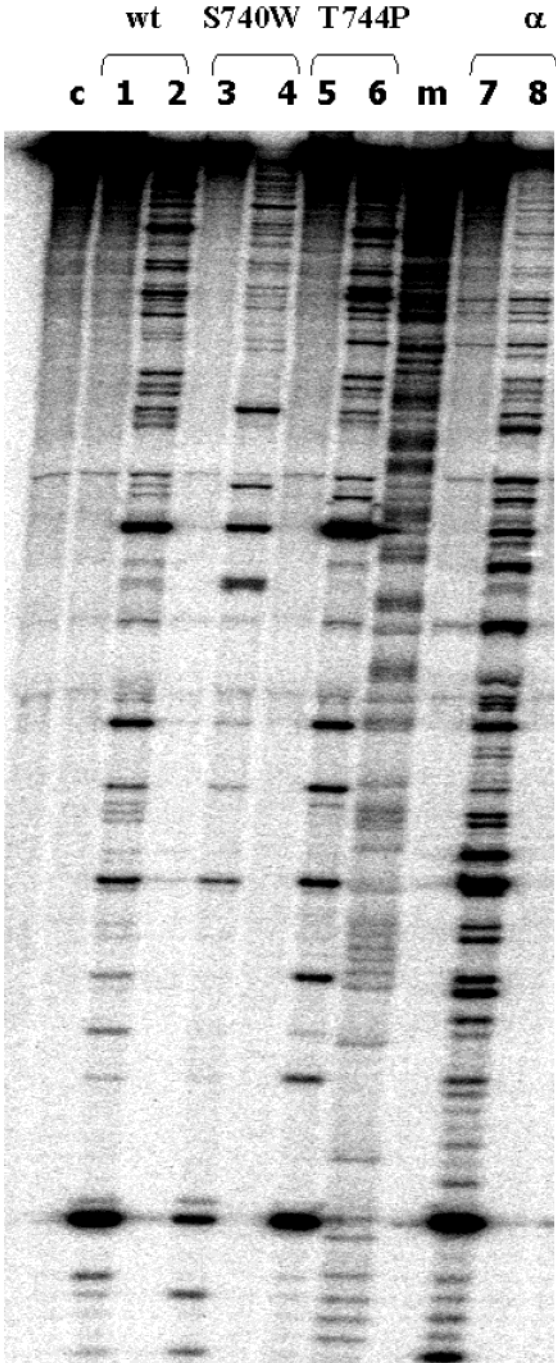


FIGURE 2: Comparison of yTop2 enzymes to hsTop2 α in the presence of VM-26. A 5'-end labeled DNA fragment was incubated with the enzymes at similar activity for 20 min at 30 °C and then stopped with SDS and proteinase K. DNA fragmentation was then evaluated with sequencing gels. Lanes: C, control DNA; 1, 3, 5, and 7, no drugs; 2, 4, 6, and 8, with 50 μ M VM-26; m, purine marker. Wt, wild-type yeast top2; S740W, S740W mutant yeast top2; T744P, T744P mutant yeast top2; α , human top2 α .

specific sites (indicated by asterisks in Figure 4) relative to the other studied anthracyclines with wt yeast Top2. The results confirmed the observations made with agarose gels, documenting that S740W and T744P mutations confer resistance to the studied anthracyclines (Figure 4). However, T744P was completely resistant to IDA and da-IDA but not to dh-IDA-OH. The reduction of cleaved DNA fragments with T744P in comparison with wt Top2 was clearly lower with dh-IDA-OH than with the other studied anthracyclines

Table 1: Summary of Altered Poison Sensitivity of the Studied Yeast Top2 Mutations^a

	S740W	T744P	ref
VM-26/VP-16	++	=	19
quinolones	—	++	22, 24
<i>m</i> -AMSA	—/=	+	19
mitoxantrone	—/=	+/=	22, 24
IDA	—	—	this work
dh-IDA-OH	—	—/=	this work
da-IDA	—	—	this work

^a Key: ++, hypersensitive; +, more drug-sensitive than wt enzyme; =, wt sensitivity to the drug; —/=, partially drug resistant; —, completely drug resistant.

(see sites marked with arrows in Figure 4). Drug-stimulated cleavage intensity patterns were not changed by T744P mutation in the case of dh-IDA-OH, whereas they were different for *m*-AMSA and VM-26 (Figure 4), in agreement with the knowledge that both 744 and 740 residues affect sequence specificity of enzyme alone as well as *m*-AMSA and VM-26 (21, 22).

The two yTop2 mutants have been investigated previously, and the drug-sensitivity phenotypes are summarized in Table 1. The mutants displayed distinct patterns of in vitro sensitivity to poisons. The present results on anthracycline analogues show that the resistance degree of a particular Top2 mutant can be different for closely related poisons, thus suggesting that subtle structural changes of target as well as drugs can affect poison activity against Top2. Interestingly, T744P is uniquely resistant to anthracyclines (Table 1).

Modeled Covalent Top2–DNA Complex. Top2 undergoes marked conformational modifications during the catalytic process and transports a DNA duplex through a cut in another, driven by nucleotide binding and hydrolysis (9). Unfortunately, nowadays the three-dimensional structure of a covalent Top2–DNA complex is still blurred. As explicitly described into the Experimental Procedures, we have then modeled an hypothetical topology of the covalent Top2–DNA complex by using the Berger/Wang crystal coordinates (18). As shown in Figure 5, the general architecture of the Top2 enzyme is compatible with available crystallographic structures (9). It is still clearly possible to recognize head, shoulder, arm, and elbow domains. Two groups of amino acids seem to be directly involved in the interaction with the double helix of the DNA: from Tyr734 to Thr744 and from Lys775 to Tyr782. In particular, the region between Tyr734 to Thr744 is localized closely to the cleaved DNA strand (between +1 and –1 position). Interestingly, both mutants experimentally considered in the present study, S740W and T744P, are localized in this region. Consequently, we have explored the possibility that this particular region at the interface between the cleaved DNA and Top2 may represent the hypothetical recognition site of the studied antitumor compounds.

Putative Anthracycline Binding Site in Top2–DNA Cleavable Complex. Starting from the coordinates of our modeled covalent Top2–DNA complex, a molecular docking study has been carried out to analyze the possible interactions of anthracycline drugs with the Top2–DNA complex at the DNA cleavage site. We first modeled interactions of anthracyclines with the cleavable complex by investigating the

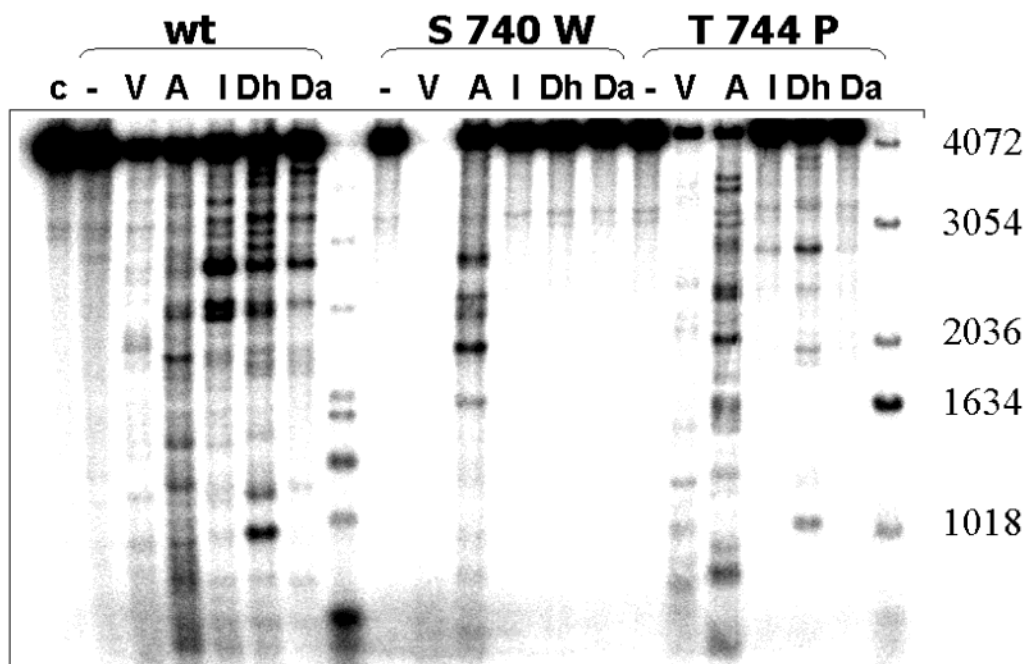


FIGURE 3: Sensitivity of yTop2 mutants to anthracycline analogues with a double-strand DNA cleavage assay. A Simian virus 40 *EcoRI*–*BclI* DNA fragment was uniquely 5′-end labeled and incubated with enzymes and drugs for 20 min at 30 °C and then stopped with SDS and proteinase K. DNA double-strand cleavage was then evaluated by agarose gel electrophoresis. Lanes: C, control DNA; –, no drugs; V, 20 μM VM-26; A, 10 μM *m*-AMSA; I, 1 μM IDA; Dh, 10 μM dh-IDA-OH; Da, 10 μM da-IDA. Lanes without labels are molecular weight markers. On top of the gel: wt, wt yTop2; S740W, yeast S740W mutant top2; T744P, yeast T744P mutant top2. On the right, the numbers indicate molecular weight of markers.

parent drug DOX and wt Top2. DOX interactions with Top2–DNA complex led to a stacking interaction of an intercalated drug molecule between +1/–1 base pairs (Figure 6). The quinone-based chromophore is accommodated perpendicular to the direction of hydrogen bonds of base pairs while the glucoside portion of the anthracycline is accommodated in the DNA minor groove contacting base pairs at positions –1 and –2. Several structural factors appear to play a role in the stabilization of the Top2–DNA–drug complex. The anthracycline is stabilized by hydrogen bonds with both DNA and Top2 and by stacking π -bond interactions between the electron-deficient quinone-based chromophore and the electron-rich purine–pyrimidine bases. Interestingly, the α 4-helix of the CAP-like domain of the wt Top2 contacts directly a DOX molecule with two strong hydrogen bonding interactions of the OH groups of Ser-740 and Thr-744 side chains with the C-12 carbonyl oxygen and the C-11 hydroxyl group of the anthraquinone moiety (Figure 6). Moreover, a third hydrogen bond is formed between the hydroxyl group at C-14 with the amide moiety of the Gln-750 side chain, which lies close to one end of the α 4-helix of the CAP-like domain. This hydrogen bond is particularly interesting since it involves a hydroxyl group that distinguishes DNR, IDA, and da-IDA from DOX and dh-IDA-OH (Figures 1 and 7). Overall, these results indicate that three amino acid residues (Ser-740, Thr-744, and Gln-750) may play a critical role in receptor recognition by anthracyclines.

Hydrogen bonds are also formed between DNA and DOX involving ring A and the daunosamine moieties (Figure 6). An hydrogen bond is formed between the drug hydroxyl group at C-9 on ring A and the base complementary to base at –1 position (a guanine in our model, Figure 6). This interaction may be a critical determinant of drug–target

stabilization since an anthracycline analogue lacking the hydroxyl group at C-9 on the right side of ring A was shown to have reduced cytotoxic activity (32). The daunosamine moiety accommodated in the DNA minor groove form two important hydrogen bonds that may contribute to DNA recognition by the compound (8). Both the amino group at 3′ position and the hydroxyl group at 4′ position of the sugar moiety are bound through hydrogen bonding with C-1 and G-2, respectively (Figure 6).

Finally, epimerization at the 4′ sugar position (epirubicin, 4′epiDOX) can nicely fit into our model, maintaining all the most crucial stabilizing interaction (as shown in Figure 7A). Accordingly, the chirality of the 4′-position can be changed without great loss of activity (33–35). On the other hand, the protonated 3′-amino group sits in front of the nucleotide at the –2 position, interacting with the corresponding base and ribose moieties through electrostatic interactions (Figure 7).

Analyzing our model of the Top2–DNA–DOX ternary complex, Thr744 and Ser740 form strong hydrogen bonding interactions with structural groups of the anthraquinone moiety, thus suggesting that the loss of these interactions (as in the studied S740W and T744P Top2 mutants) may decrease significantly the affinity of DOX for the putative receptor in the binary complex. Moreover, the replacement of Ser-740 with a more bulky Trp residue appears to greatly affect drug interactions since the indole ring of Trp is located between +1/–1 DNA bases, very likely limiting the intercalation of the anthraquinone chromophore or any other planar structure into DNA. The mutation has indeed been shown to be critical for all Top2 poisons characterized by an intercalative mode of interaction with DNA (19).

Putative m-AMSA Binding Site in Top2–DNA Cleavable Complex. We have also modeled *m*-AMSA interaction with the binary Top2–DNA complex at the DNA cleavage site

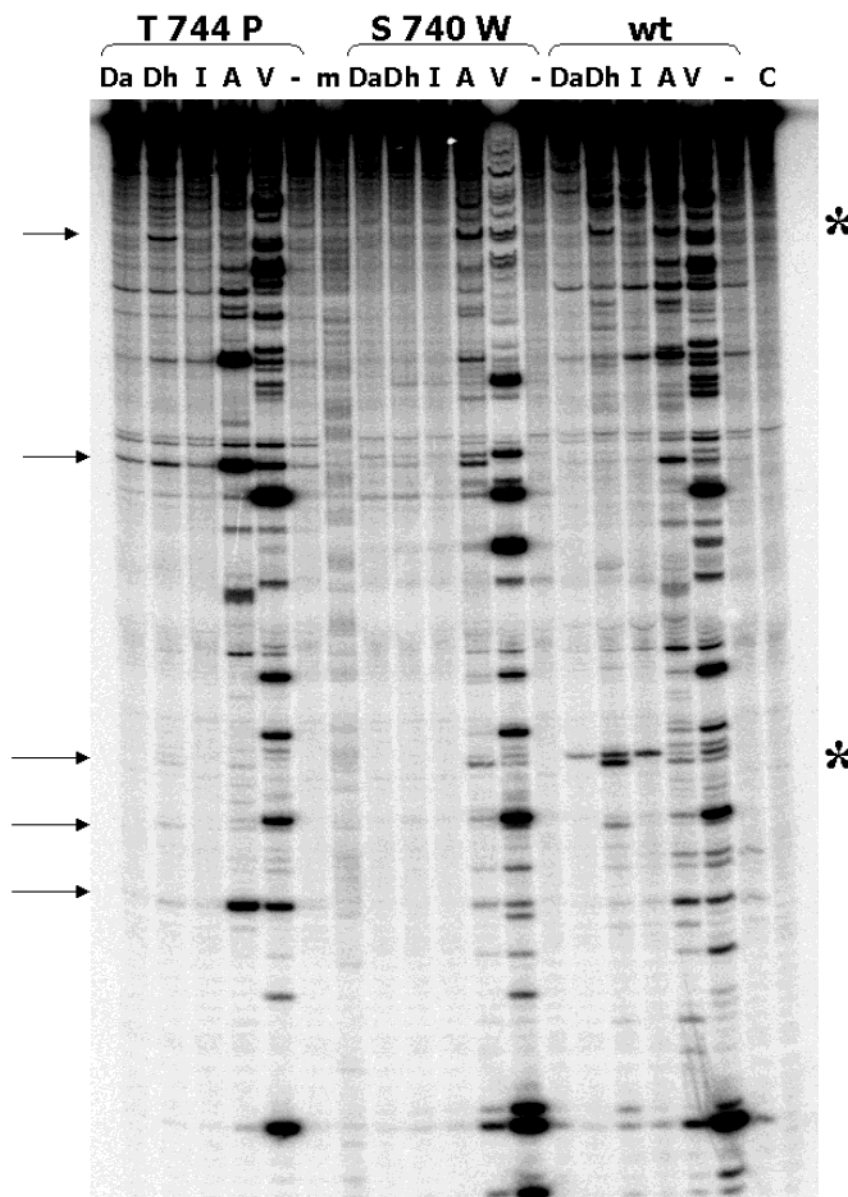


FIGURE 4: Sensitivity of yTop2 mutants to anthracycline analogues as tested in sequencing gels. A Simian virus 40 DNA fragment was uniquely 5'-end labeled at the *Eco*RI site and incubated with enzymes and drugs for 20 min at 30 °C and then stopped with SDS and proteinase K. DNA cleavage was then evaluated by sequencing gels. Lanes: C, control DNA; —, no drugs; V, 20 μ M VM-26; A, 10 μ M *m*-AMSA; I, 1 μ M IDA; Dh, 10 μ M dh-IDA-OH; Da, 10 μ M da-IDA; m, purine markers. On top of the gel: wt, wt yTop2; S740W, yeast S740W mutant top2; T744P, yeast T744P mutant top2. Arrows on the left indicate sites of DNA cleavage produced by the 744 top2 mutant with dh-IDA-OH.

(Figure 8) to be compared with the DOX receptor model. In the model, the acridine moiety, intercalated between +1/−1 DNA base pairs, is aligned with its major axis bisecting the angle between the hydrogen bonds of the sandwiching base pairs. The helix axis passes through the middle of the central acridine ring, thus the acridine chromophore is enveloped by a base pair on either side (Figure 8). As a result of *m*-AMSA intercalation, the GC and CG base pairs “buckle” by about 9° and 15°, respectively, to prevent excessive van der Waal's contacts and are separated by a nominal distance of 3.4–6.8 Å to accommodate the drug.

The strong drug–target interactions shown by the model are different from those found in the case of DOX. The hydroxyl group of Thr744 is strongly linked to the sulfonamide moiety at the 1' position on the aniline, and a second strong interaction occurs between the oxygen of the carbonyl group of Gly747 and the NH of the same sulfonamide

moiety (Figure 8). Moreover, a hydrophobic interaction is present between the side chain of Phe754 and the methyl group of the methoxy substituent at the 3' position on the aniline. When considering the structural inactive conformer, *o*-AMSA, computer models suggest that a repulsive steric interaction occurs between the methoxy substituent at the 2' position and both DNA and Top2 structures, in particular Phe752 and the base in −1 position (data not shown). This may constitute a structural basis for the requirement of the substituent at the 1' position on the aniline ring for *m*-AMSA activity.

Effects of S740W and T744P mutations may differently affect *m*-AMSA interactions in the complex. As observed for DOX, the replacement of Ser740 with the more bulky Trp affects the binding of *m*-AMSA to its receptor by completely preventing entrance of drugs to the site (not shown). The second mutation is known to confer hypersen-

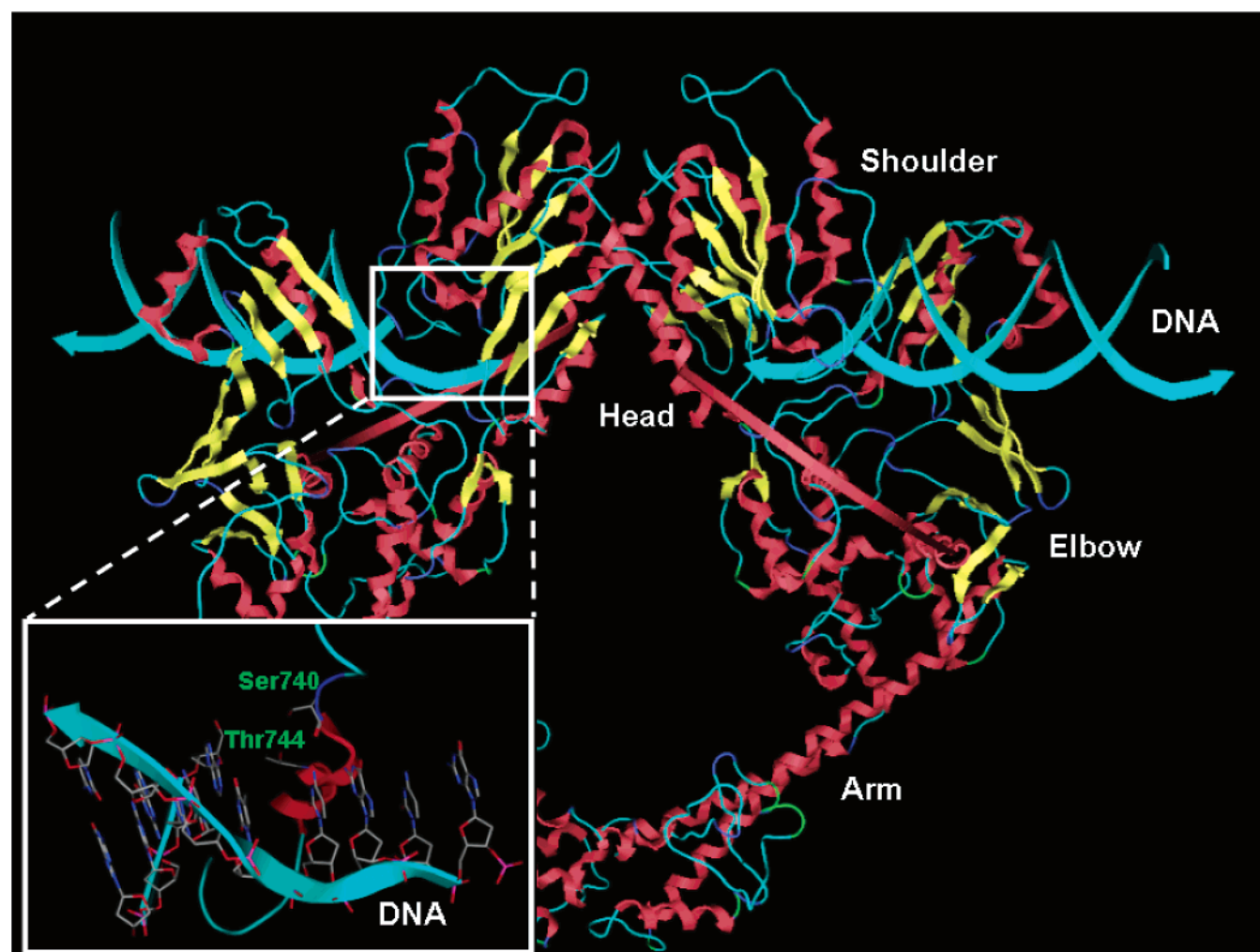


FIGURE 5: Modeled topology of the covalent Top2–DNA complex. The model shows the two yeast enzyme subunits each bound to a DNA duplex and has been constructed from the Berger/Wang crystal coordinates (18). On the bottom left corner, it is shown the molecular details of the +1/-1 DNA bases and the relative positions of Ser740 and Thr744 of the Top2 CAP-like domain. The model figure has been prepared with the MOE software, and main portions of the complex are indicated.

sitivity to *m*-AMSA (19) that has been suggested to be not necessarily associated with an increased affinity of the drug for its target (24). Since Thr744 lies in the middle of helix $\alpha 4$ of the Top2 helix–turn–helix domain (CAP domain), a Pro can disrupt the helical secondary structure changing the stability of the protein–DNA complex and, consequently, affect the cleavage/religation equilibrium to favor the cleaved state (24). We have then modeled the T744P mutation in the case of *m*-AMSA, and interestingly, the expected loss of the strong hydrogen-bonding interaction between hydroxyl group of Thr744 and the drug sulfonamide moiety was completely replaced by another strong hydrogen bond between NH_2 group of Asn756 and the same sulfonamide moiety (data not shown). Therefore, the results suggest that no hydrogen bond may be lost with T744P mutation, and this may contribute to the observed higher sensitivity of the mutant.

DISCUSSION

In the present paper, we propose a putative model of an anthracycline interaction site in the Top2–DNA cleavable complex based on DNA cleavage assays and computer simulation. The model indicates that an anthracycline molecule may interact with DNA strands at the cleavage site

by intercalating between base pairs at -1 and $+1$ positions of the single-stranded region as well as with the $\alpha 4$ helix of the CAP-like domain of Top2. Moreover, crucial hydrogen bonds are suggested to form between the aromatic ring moiety of the drug and specific amino acid residues that, when mutated, confer enzyme resistance to anthracyclines. The present model, based on both computer simulations and biochemical findings, is consistent with many known structure–activity relationships of anthracyclines and may thus represent a basis to further understand the drug Top2 poisoning activity.

Our model has been built from a particular conformation state of Top2, the Berger/Wang X-ray crystal structure of yeast Top2 (18). Since Top2 conformation very likely changes during catalysis, it is possible that additional interactions critical for anthracycline activity occur with other conformations (36). Different enzyme conformations have been found in different crystals likely representing diverse transient conformations of Top2 during the catalytic cycle. The GyrA structure (37) likely represents a precleavage conformation of type II topoisomerases. However, the gyrA crystal lacks the B' domain that would need to be modeled before docking in a DNA and then a drug molecule. This would add further uncertainties to the final drug receptor

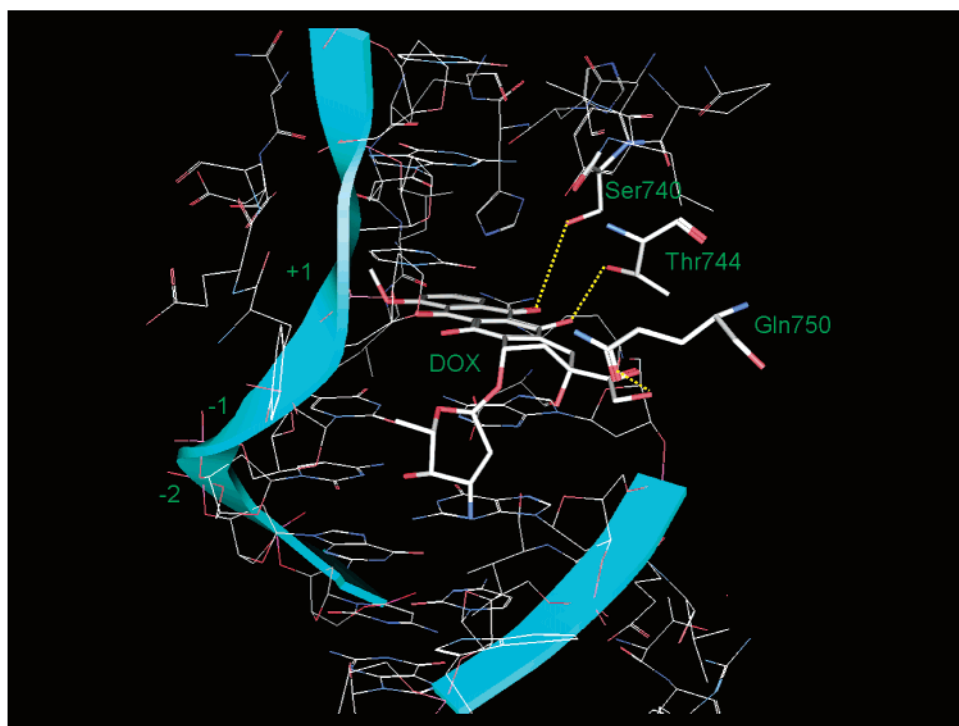


FIGURE 6: Putative receptor of DOX the binary Top2–DNA complex. A DOX is intercalated into the +1/–1 DNA bases (see text for experimental details). DNA strand backbones are indicated by light blue ribbons. Amino acids forming hydrogen bonds with DOX and DNA bases adjacent to the cleaved site are indicated with green labels. Ser740, Thr744, Gln750 and drug molecule are shown in bold sticks. Hydrogen atoms are not shown, and hydrogen bonds are indicated by yellow lines.

model. The Berger/Wang structure is indicated as an open conformation of γ Top2 with a broken G DNA segment (18), whereas the Fass/Berger structure may represent an intermediate step between a precleavage and an open conformation (36). Thus, the former has been used to model drug interaction with Top2–DNA complex by us and others (22) since it can likely be the molecular target of agents that stimulate Top2-mediated DNA breaks. Our model predicts that anthracyclines interact with the CAP-like domain α 4 helix that is not involved in DNA transport, which is likely due to the Top2 B' domain (18). This may suggest that anthracycline interactions with the CAP-like domain α 4 helix may be maintained during other catalytic steps with minor modifications.

We have built a molecular model of a Top2–polyCG covalent complex that is in agreement with previous reports (22, 36, 38). The optimized model has then been used, through a flexible docking methodology, to identify the most stable conformer of DOX structure into the enzyme–DNA covalent complex. In the model (Figure 6), the planar moiety of the DOX molecule is squeezed between the layers of C–G base pairs of the cleaved B-DNA with its long axis that is almost perpendicular to the direction of base pair hydrogen bonds. In such a structure, the drug sugar is placed in the DNA minor groove, and ring D of the anthracycline molecule protrudes into the DNA major groove, in agreement with X-ray structures of DOX intercalated into the double helix (39). Moreover, cyclohexene ring A of the aglycon is almost planar, with the exception of C-9, which is displaced in the same direction as the amino sugar relative to the plane of the aglycon. The hydroxyl O-9 is involved in a hydrogen bond with the nitrogen atom of the guanine at position –1, therefore suggesting a structural

basis for much reduced cytotoxicity of an analogue lacking the 9-OH group (32).

As shown by the model, the molecular arrangement gives rise to other specific hydrogen-bonding interactions that stabilize drug binding to the target. Interestingly, DOX contacts the CAP-like domain of Top2: Ser-740 and Thr-744 residues form two strong hydrogen-bonding interactions with a carbonyl oxygen (C-12) and a hydroxyl group (C-11) of the anthraquinone moiety. According to DNA cleavage results, both amino acids seem to play a critical role in the anthracycline recognition process. According to our model, the removal of the C-11 hydroxyl group would prevent the formation of the hydrogen bonding, and it indeed results in a loss of drug activity against Top2 as well as of drug cell killing activity (33, 34). The critical role in specific drug–target interactions of both hydroxyl groups at C-11 and C-9 were indicated at the early time of structure–activity relationship investigations of drug-stimulated DNA cleavage in cultured cells and with purified murine Top2 (see Figure 5 in ref 35). A third hydrogen bonding is seen on the other side of the aglycon ring system involving the C-14 oxygen atom and the side chain of glutamine 750. The C-14 OH group is present in dh-IDA-OH but not in IDA and da-IDA analogues. We may note that the T744P mutation is completely resistant to the latter while it is partially resistant to the former, suggesting that the mutation has a less severe effect if two hydrogen bonds, instead of only one, are preserved. Thus, the three hydrogen-bonding interactions between the CAP-domain α 4 helix and the drug aromatic ring system may serve as an anchor for the DOX molecule into the ternary cleavable complex. In addition to the stacking forces at the intercalation site, these hydrogen bonds may considerably contribute to the complex stability, likely

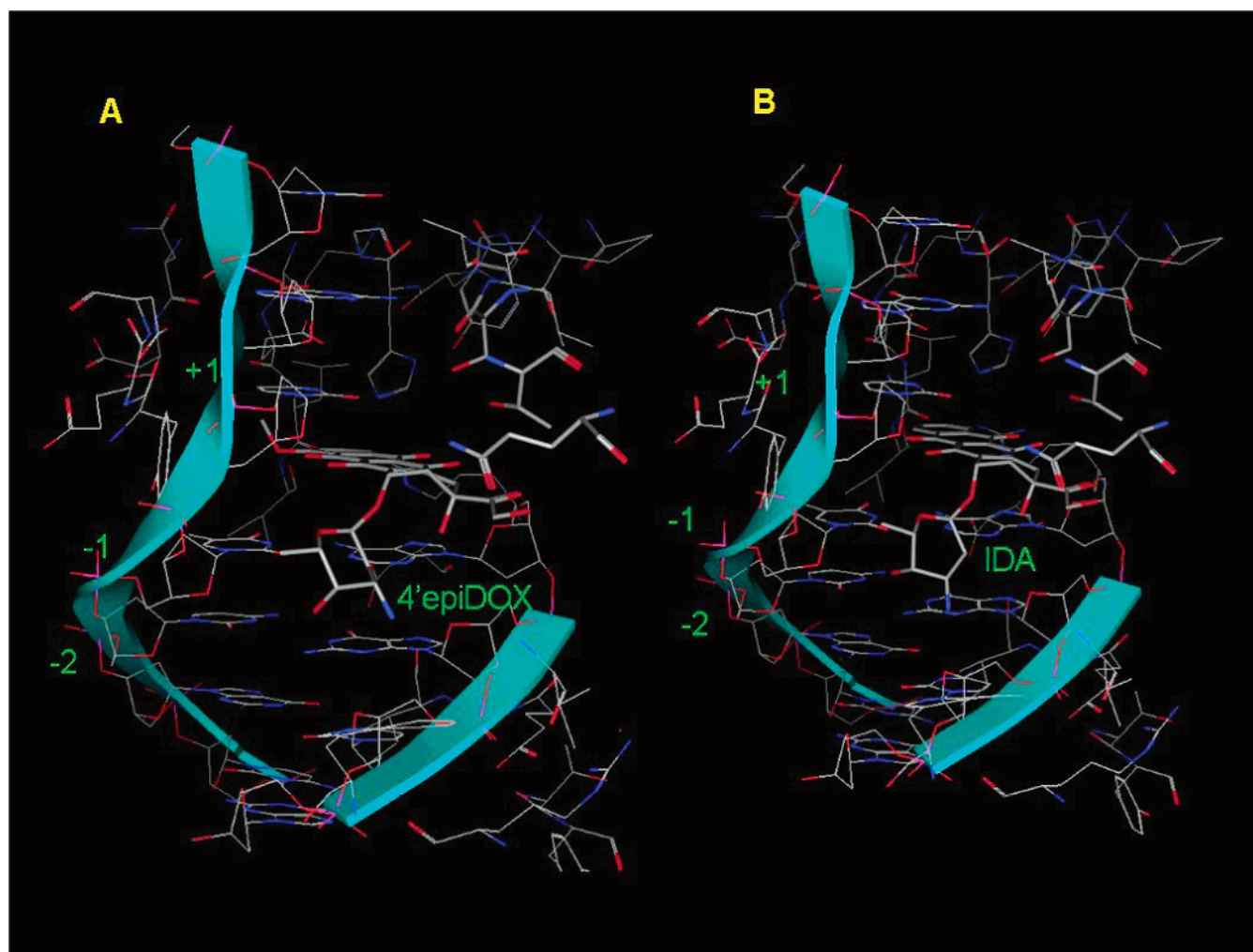


FIGURE 7: Docking of DOX and DNR derivatives into the receptor model. Putative interactions of 4'epiDOX (epirubicin, left) and IDA (4-demethoxyDNR, right) at the anthracycline receptor in the Top2–DNA complex. Crucial amino acid residues are underlined. Hydrogen atoms are not shown, and hydrogen bonds are indicated by yellow lines.

preventing the annealing of cleaved strands before DNA religation.

The methoxy group at C-4 of ring D of anthracyclines is not required for anticancer and cytotoxic activities, and IDA is indeed a highly active compound (see also below). This can be in accordance with our model, in which ring D protrudes out into the major groove and the methoxy group has no direct interaction with DNA or Top2 (Figure 7B). The anthracycline analogue carminomycin, in which the methoxy group is replaced with an OH group, has antitumor activity as well. Both the amino group at 3' position and the hydroxyl group at 4' position of the sugar moiety are bound through hydrogen bondings with C-1 and G-2, respectively. Epimerization at the 4' sugar position can nicely fit into our model, maintaining all the most crucial stabilizing interactions (as shown in Figure 7A). Accordingly, the chirality of the 4' position can be changed without great loss of activity (epirubicin, 4'-epiDOX). On the other hand, the protonated 3'-amino group sits in front of the nucleotide at the –2 position, interacting with the corresponding base and ribose moieties through electrostatic interactions. However, the removal of the amino group does not lead to a lower potency in terms of cytotoxic and Top2 poisoning activities for 4-demethoxy analogues (see for instance dh-IDA-OH) (35, 40). Thus, the presence of the cationic charge may be

necessary for derivatives with a methoxy group at C-4, which likely reduces drug activity since its removal greatly improves the drug ability to trap Top2 (34, 35). Moreover, the epimerization of the amino group is well-known to change drastically the preferred bases of anthracycline-stimulated DNA cleavage exactly at the –2 position (40), in full agreement with the present model in which the amino group can directly interact with the base pair at the –2 position.

A comparison with the interactions modeled for *m*-AMSA with the Top2–DNA complex (Figure 8) showed that different poisons may have distinct strong interactions at the receptor site, suggesting that structural basis for activity can substantially be different for unrelated compounds. Thr744Pro mutation of yeast Top2 is hypersensitive to *m*-AMSA, whereas it is resistant to anthracyclines. The model has indicated that *m*-AMSA may form a hydrogen bond with Pro, thus the mutation would not prevent the availability of other hydrogen bondings. The present findings are not in alternative to the proposed argument (24) that the mutation may alter the position of other catalytic residues so that a strong *m*-AMSA binding to the Top2–DNA complex is maintained.

Several previous studies of yTop2 mutants provided evidence for the involvement of the $\alpha 4$ helix of the CAP-

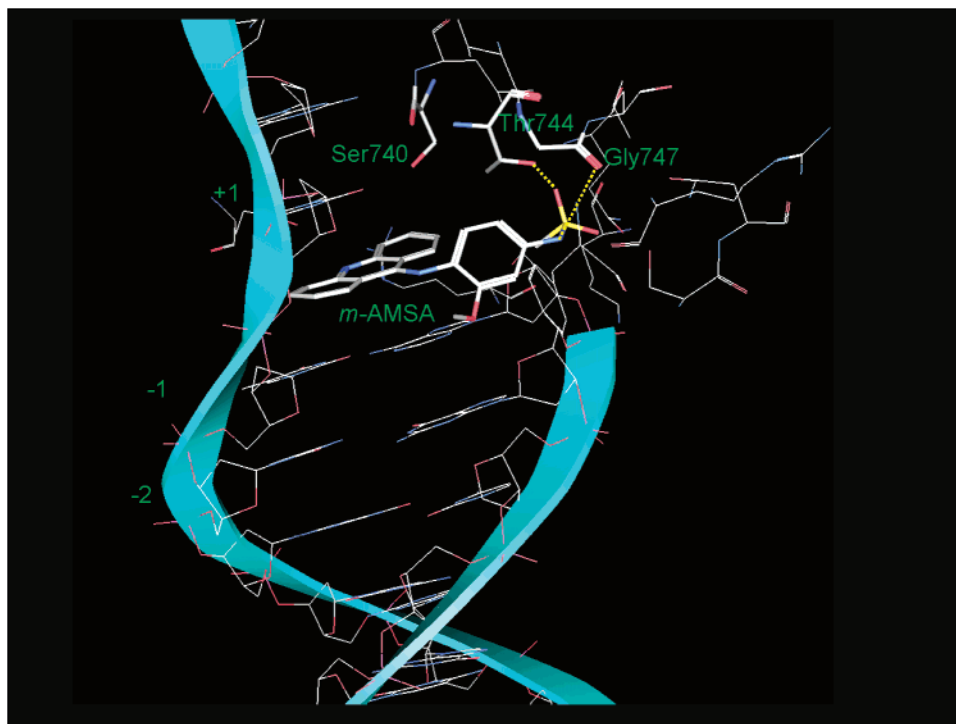


FIGURE 8: Putative receptor of *m*-AMSA in the binary Top2–DNA complex. An *m*-AMSA molecule is intercalated into the +1/–1 DNA bases (see text for experimental details). DNA strand backbones are indicated by light blue ribbons. Amino acids forming hydrogen bonds with the drug Ser740 and DNA bases adjacent to the cleaved site are indicated with green labels. Ser740, Thr744, Gly747 and drug molecule are shown in bold sticks. Hydrogen atoms are not shown, and hydrogen bonds are indicated by yellow lines.

like domain in DNA binding and drug activity (19–24). Recently, position-specific DNA breaks produced by Top2 have been demonstrated with benzo[*a*]pyrene diol epoxide adducts (13). Interestingly, adduct intercalation between positions –1 and +1 results in trapping of Top2 cleavage complexes, therefore providing a direct evidence for the stacking model originally proposed on the basis of observations with noncovalently bound intercalating anthracyclines (10). Thus, our model of an anthracycline interaction site is consistent with these findings. Whether one anthracycline molecule at one Top2 subunit can affect the cleavage activity of the other subunit cannot be predicted by our model. However, concerted cleavage activity by the two Top2 subunits has been proposed in the case of anthracycline action (41) and benzo[*a*]pyrene adducts (13). Nevertheless, non-concerted cleavage of the two DNA strands by Top2 subunits was shown by Osheroff and co-workers for VP-16 action recently (42). Thus, we can conclude that anthracyclines and other intercalating agents binding to the proposed receptor site (Figure 6) can affect both subunits of a Top2 homodimer albeit with enhanced efficiency at the binding site (13, 41).

In conclusion, our model has been built from a particular conformation state of Top2; therefore, other critical interactions may occur between anthracycline molecules and DNA–enzyme complexes. While entering its putative receptor, a drug may form other molecular contacts that need to be established to get a complete understanding of drug–target interactions. This has been shown to determine the activity and specificity of a compound targeted to a kinase (28). We also acknowledge that modeling DNA–Top2 complex first and then modeling in a compound may produce uncertainties. For example, the G-segment DNA can be distorted at the active site upon binding. We therefore let a B-DNA segment

with four single-stranded nucleotides to accommodate with the Top2 interaction region (CAP domain) and to adjust its conformation by energy minimization (see above). Nevertheless, even though drug-resistant mutations may either directly affect amino acid interactions with drugs or alter enzyme–DNA interactions indirectly affecting the drug-binding site (24), the computer-simulated anthracycline receptor is strongly consistent with the present DNA cleavage results of γ Top2 mutants as well as several published structure–activity relationships of anthracyclines. Thus, we propose that our model may represent one mode of DOX interaction within the binary Top2–DNA complex that is relevant for the biological activity of this series of compounds. The model also provides a framework for further investigations of effective Top2 poison receptors and predicts protein–drug interactions that may be tested in further investigations.

REFERENCES

1. Wang, J. C. (1996) DNA topoisomerases, *Annu. Rev. Biochem.* 65, 635–692.
2. Wang, J. C. (2002) Cellular roles of DNA topoisomerases: a molecular perspective, *Nat. Rev. Mol. Cell Biol.* 3, 430–440.
3. Pommier, Y., Pourquier, P., Fan, Y., and Strumberg, D. (1998) Mechanism of action of eukaryotic DNA topoisomerase I and drugs targeted to the enzyme, *Biochim. Biophys. Acta* 1400, 83–105.
4. Nitiss, J. L. (1994) Roles of DNA topoisomerases in chromosomal replication and segregation, *Adv. Pharmacol.* 29A, 103–134.
5. Liu, L. F. (1989) DNA topoisomerase poisons as antitumor drugs, *Annu. Rev. Biochem.* 58, 351–375.
6. Pommier, Y., Pourquier, P., Fan, Y., and Strumberg, D. (1998) Mechanism of action of eukaryotic DNA topoisomerase I and drugs targeted to the enzyme, *Biochim. Biophys. Acta* 1400, 83–105.
7. Froelich-Ammon, S. J., and Osheroff, N. (1995) Topoisomerase poisons: harnessing the dark side of enzyme mechanism, *J. Biol. Chem.* 270, 21429–21432.

8. Capranico, G., Binaschi, M., Borgnetto, M. E., Zunino, F., and Palumbo, M. (1997) A protein-mediated mechanism for the DNA sequence-specific action of topoisomerase II poisons, *Trends Pharmacol. Sci.* 18, 323–329.
9. Wang, J. C. (1996) DNA topoisomerases, *Annu. Rev. Biochem.* 65, 635–692.
10. Capranico, G., Kohn, K. W., and Pommier, Y. (1990) Local sequence requirements for DNA cleavage by mammalian topoisomerase II in the presence of doxorubicin, *Nucleic Acids Res.* 18, 6611–6619.
11. Fortune, J. M. and Osheroff, N. (2000) Topoisomerase II as a target for anticancer drugs: when enzymes stop being nice, *Prog. Nucleic Acid Res. Mol. Biol.* 64, 221–253.
12. Capranico, G., and Binaschi, M. (1998) DNA sequence selectivity of topoisomerases and topoisomerase poisons, *Biochim. Biophys. Acta* 1400, 185–194.
13. Khan, Q. A., Kohlhagen, G., Marshall, R., Austin, C. A., Kalena, G. P., Kroth, H., Sayer, J. M., Jerina, D. M., and Pommier, Y. (2003) Position-specific trapping of topoisomerase II by benzo-[a]pyrene diol epoxide adducts: implications for interactions with intercalating anticancer agents, *Proc. Natl. Acad. Sci. U.S.A.* 100, 12498–12503.
14. Redinbo, M. R., Stewart, L., Kuhn, P., Champoux, J. J., and Hol, W. G. (1998) Crystal structures of human topoisomerase I in covalent and noncovalent complexes with DNA, *Science* 279, 1504–1513.
15. Staker, B. L., Hjerrild, K., Feese, M. D., Behnke, C. A., Burgin, A. B., Jr., and Stewart, L. (2002) The mechanism of topoisomerase I poisoning by a camptothecin analog, *Proc. Natl. Acad. Sci. U.S.A.* 99, 15387–15392.
16. Nitiss, J. L. (1998) Investigating the biological functions of DNA topoisomerases in eukaryotic cells, *Biochim. Biophys. Acta* 1400, 63–81.
17. Walker, J. V., and Nitiss, J. L. (2002) DNA topoisomerase II as a target for cancer chemotherapy, *Cancer Invest.* 20, 570–589.
18. Berger, J. M., Gamblin, S. J., Harrison, S. C., and Wang, J. C. (1996) Structure and mechanism of DNA topoisomerase II, *Nature* 379, 225–232.
19. Hsiung, Y., Elsea, S. H., Osheroff, N., and Nitiss, J. L. (1995) A mutation in yeast TOP2 homologous to a quinolone-resistant mutation in bacteria. Mutation of the amino acid homologous to Ser83 of *Escherichia coli* gyrA alters sensitivity to eukaryotic topoisomerase inhibitors, *J. Biol. Chem.* 270, 20359–20364.
20. Strumberg, D., Nitiss, J. L., Rose, A., Nicklaus, M. C., and Pommier, Y. (1999) Mutation of a conserved serine residue in a quinolone-resistant type II topoisomerase alters the enzyme-DNA and drug interactions, *J. Biol. Chem.* 274, 7292–7301.
21. Strumberg, D., Nitiss, J. L., Dong, J., Kohn, K. W., and Pommier, Y. (1999) Molecular analysis of yeast and human type II topoisomerases. Enzyme-DNA and drug interactions, *J. Biol. Chem.* 274, 28246–28255.
22. Strumberg, D., Nitiss, J. L., Dong, J., Walker, J., Nicklaus, M. C., Kohn, K. W., Heddle, J. G., Maxwell, A., Seeber, S., and Pommier, Y. (2002) Importance of the fourth alpha-helix within the CAP homology domain of type II topoisomerase for DNA cleavage site recognition and quinolone action 2, *Antimicrob. Agents Chemother.* 46, 2735–2746.
23. Hammonds, T. R., Foster, S. R., and Maxwell, A. (2000) Increased sensitivity to quinolone antibacterials can be engineered in human topoisomerase IIalpha by selective mutagenesis, *J. Mol. Biol.* 300, 481–491.
24. Dong, J., Walker, J., and Nitiss, J. L. (2000) A mutation in yeast topoisomerase II that confers hypersensitivity to multiple classes of topoisomerase II poisons, *J. Biol. Chem.* 275, 7980–7987.
25. Critchlow, S. E., and Maxwell, A. (1996) DNA cleavage is not required for the binding of quinolone drugs to the DNA gyrase–DNA complex, *Biochemistry* 35, 7387–7393.
26. Patel, S., Sprung, A. U., Keller, B. A., Heaton, V. J., and Fisher, L. M. (1997) Identification of yeast DNA topoisomerase II mutants resistant to the antitumor drug doxorubicin: Implications for the mechanisms of doxorubicin action and cytotoxicity, *Mol. Pharmacol.* 52, 658–666.
27. Cornarotti, M., Tinelli, S., Willmore, E., Zunino, F., Fisher, L. M., Austin, C. A., and Capranico, G. (1996) Drug sensitivity and sequence specificity of human recombinant DNA topoisomerases IIalpha (p170) and IIbeta (p180), *Mol. Pharmacol.* 50, 1463–1471.
28. Moro, S., and Jacobson, K. A. (2002) Molecular modeling as a tool to investigate molecular recognition in P2Y receptors, *Curr. Pharm. Des.* 8, 2401–2413.
29. Halgren, T. A. (1996) Merck molecular force field. I–V, *J. Comput. Chem.* 17, 490–641.
30. Halgren, T. A. (1999) Merck molecular force field. VI–VII, *J. Comput. Chem.* 20, 720–748.
31. Binaschi, M., Farinosi, R., Borgnetto, M. E., and Capranico, G. (2000) In vivo site specificity and human isoenzyme selectivity of two topoisomerase II-poisoning anthracyclines, *Cancer Res.* 60, 3770–3776.
32. Capranico, G., De Isabella, P., Penco, S., Tinelli, S., and Zunino, F. (1989) Role of DNA breakage in cytotoxicity of doxorubicin, 9-deoxydoxorubicin, and 4-demethyl-6-deoxydoxorubicin in murine leukemia P388 cells, *Cancer Res.* 49, 2022–2027.
33. Capranico, G., Soranzo, C., and Zunino, F. (1986) Single-strand DNA breaks induced by chromophore-modified anthracyclines in P388 leukemia cells, *Cancer Res.* 46, 5499–5503.
34. Capranico, G., Zunino, F., Kohn, K. W., and Pommier, Y. (1990) Sequence-selective topoisomerase II inhibition by anthracycline derivatives in SV40 DNA: relationship with DNA binding affinity and cytotoxicity, *Biochemistry* 29, 562–569.
35. Zunino, F., and Capranico, G. (1990) DNA topoisomerase II as the primary target of anti-tumor anthracyclines, *Anticancer Drug Des.* 5, 307–317.
36. Fass, D., Bogden, C. E., and Berger, J. M. (1999) Quaternary changes in topoisomerase II may direct orthogonal movement of two DNA strands, *Nat. Struct. Biol.* 6, 322–326.
37. Morais Cabral, J. H., Jackson, A. P., Smith, C. V., Shikotra, N., Maxwell, A., and Liddington, R. C. (1997) Crystal structure of the breakage-reunion domain of DNA gyrase, *Nature* 388, 903–906.
38. Liu, Q., and Wang, J. C. (1999) Similarity in the catalysis of DNA breakage and rejoining by type IA and IIA DNA topoisomerases, *Proc. Natl. Acad. Sci. U.S.A.* 96, 881–886.
39. Quigley, G. J., Wang, A. H. J., Ughetto, G., VanDerMarel, G., vanBoom, J. H., and Rich, A. (1980) Molecular structure of an anticancer drug–DNA complex: Daunomycin plus d(CpGpTpApCpG), *Proc. Natl. Acad. Sci. U.S.A.* 77, 7204–7208.
40. Capranico, G., Butelli, E., and Zunino, F. (1995) Change of the sequence specificity of daunorubicin-stimulated topoisomerase II DNA cleavage by epimerization of the amino group of the sugar moiety, *Cancer Res.* 55, 312–317.
41. Bigioni, M., Zunino, F., and Capranico, G. (1994) Base mutational analysis of topoisomerase II–idarubicin–DNA ternary complex formation. Evidence for enzyme subunit cooperativity in DNA cleavage, *Nucleic Acids Res.* 22, 2274–2281.
42. Bromberg, K. D., Burgin, A. B., and Osheroff, N. (2003) A two-drug model for etoposide action against human topoisomerase IIalpha, *J. Biol. Chem.* 278, 7406–7412.

B10361665